Pakistan Veterinary Journal

ISSN: 0253-8318 (PRINT), 2074-7764 (ONLINE)
DOI: 10.29261/pakvetj/2024.138

RESEARCH ARTICLE

Antibacterial Activity of Laser Ablated Gold and Hydroxyapatite Nanoparticles Conjugated Cefuroxime against *Staphylococcus saprophyticus*

Hadeel M Yosif[1], Buthenia A Hasoon[1], Majid S Jabir[1*], Syed Hilal Yaqoob[2], Haney Samir[3,4] and Ayman A Swelum[5*]

[1]Department of Applied Science, University of Technology- Iraq; [2]Division of Animal Biotechnology, Faculty of Veterinary Sciences, SKUAST -Kashmir Shuhama Srinagar J&K India; [3]Department of Theriogenology, Faculty of Veterinary Medicine, Cairo University, Egypt; [4]Department of Veterinary Medicine, Tokyo University of Agriculture and Technology, Japan; [5]Department of Animal Production, College of Food and Agriculture Sciences, King Saud University, Riyadh, Saudi Arabia
*Corresponding author: 100131@uotechnology.edu.iq (MSJ); aswelum@ksu.edu.sa (AAS)

ARTICLE HISTORY (23-445)

Received: October 1, 2023
Revised: January 5, 2024
Accepted: January 9, 2024
Published online: March 18, 2024

Key words:
Laser ablation
Hydroxyapatite NPs
Au NPs
Cefuroxime
Staphylococcus saprophyticus

ABSTRACT

A frequent and efficient weapon in the fight against infectious diseases is antibiotics. Antimicrobial resistance, however, has emerged as a major concern in public health due to the unintentional, overuse, and improper administration of antibiotics. In the current study, a heterostructure of gold (Au), Hydroxyapatite (HAP) and Cefuroxime was produced using an environmentally friendly pulsed laser ablation technique to improve the antibacterial activity of Cefuroxime against *Staphylococcus* (*S.*) *saprophyticus*. X-ray diffraction (XRD), Fourier transforms infrared spectroscopy, UV/Vis spectrophotometry, and field emission-scanning electron microscopy (FE-SEM) were used to characterize the heterostructure nanocomposite. The susceptibility of *S. saprophyticus* to the Au-Hydroxyapatite-Cefuroxime was evaluated in terms of preventing biofilm development in the urinary catheter. This study confirmed the greater antimicrobial activity of hetero nanocomposite of the Hydroxyapatite-Cefuroxime-AuNPs than Cefuroxime alone against *S. saprophyticus*. The Hydroxyapatite nanoparticles (NPs)-Cefuroxime-Gold nanoparticles (AuNPs) hybrid was developed as an intelligent drug delivery mechanism to prevent the proliferation of *S. saprophyticus* and to hinder the formation of bacterial biofilm on Foley catheters. The smart hetero nanocomposite has shown a promising result, which could be a reliable therapy against *S. saprophyticus* in the future and could be used as a promising approach for succeeding bacterial biofilm inhibition during urinary tract infection.

To Cite This Article: Yosif HM, Hasoon BA, Jabir MS, Yaqoob SH, Samir H and Swelum AA, 2024. Antibacterial activity of laser ablated gold and hydroxyapatite nanoparticles conjugated cefuroxime against staphylococcus saprophyticus. Pak Vet J, 44(1): 38-46. http://dx.doi.org/10.29261/pakvetj/2024.138

INTRODUCTION

Non-aureus *Staphylococcus* (*S.*) represent the most significant and widely distributed categories of disease-causing agents in lactating dairy cows and include numerous species such as *Staphylococcus haemolyticus*, *S. chromogenes*, *S. saprophyticus*, *S. sciuri*, *S. simulans*, *S. epidermidis*, and *S. succinus* (Wald *et al.*, 2019; De Buck *et al.*, 2021; Ahmed *et al*., 2022). Nanotechnology and nano-delivery systems are modern scientific fields that deal with the development, characterization, manufacture, and utilization of nanoscale (1–100 nm) materials, systems, and devices (Naima *et al*., 2022). In the field of cosmetics and cosmeceuticals, where nanotechnology is acknowledged as one of the revolutionizing technologies, substantial research has been done (Raj *et al.*, 2012; Kaul *et al.*, 2018).

The majority of mammalian diseases are thought to be caused by bacterial infections (Cassandra, 2017). One of the key developments in modern medicine is the discovery of antibiotics (Makabenta *et al.*, 2021). However, the misuse of antibiotics in both clinic and non-clinic has resulted in the emergence of numerous superbugs/bacterial pathogens that are resistant to many different types of antibiotics, such as vancomycin-resistant *S. aureus* (VISA) and methicillin-resistant *S. aureus* (MRSA) (Willyard, 2017; Naylor *et al.*, 2018; Liu *et al*., 2023). Bacteria remain one of the chief risks to health as a result. To prevent bacterial growth and even kill bacteria, scientists have created several antimicrobial drugs. As of now, natural antibacterial agents, inorganic antibacterial agents and organic antibacterial agents make up the majority of the regularly utilized antibacterial agents (Vila *et al*., 2020).

The broad range and availability of antibacterial products are expanding, which leads to an increase in antimicrobial resistance and major environmental issues (Patel *et al.,* 2021; Abbas *et al*., 2022). Therefore, it is critical to create potent antibacterial materials to replace these medications. A new route for antibacterial medications has been made possible by the quick growth of nanoscience and technology and the continual development of science and technology. Since it contains a mineral that is similar to that found in the skeleton, Hydroxyapatite (HAP), is often used in medical studies. It is known for its superior biocompatibility, high levels of bioactivity, osteoconductivity, and capacity for chemical stability, all of which make it advantageous in this field. To create HAP-based composites, various polymers or ceramics are combined to boost the mechanical properties. Hydroxyapatite exhibits poor antibacterial effects, which prompts research on modifying bacteriostatic ions, including Sr, Zn, Ce and Au (Tian *et al.,* 2016; Zhang *et al.,* 2016; Yuan *et al.,* 2018).

The bactericidal characteristics activity of metallic nanoparticles depends on their size, in general, they produce more ions when they are presented at micro or macro scales (Silva-Holguín and Reyes-López, 2020). They are less cytotoxic and have unique optical characteristics. Gold nanoparticles (AuNPs) are frequently used in different biomedical research applications, such as biomedical imaging and biosensors (Hassan *et al.*, 2022). Beta-lactam antibiotics such as cephalosporins are used to treat both Gram-positive and Gram-negative bacteria-caused illnesses across a variety of conditions (Zhang *et al.,* 2000).

Urinary tract infections (UTIs) are among the most common bacterial infections and affect about 150 million individuals annually worldwide (Mancuso *et al*., 2023). UTIs may be caused by both Gram-positive and Gram-negative bacteria like *Escherichia coli, Enterococcus* spp., *Klebsiella pneumoniae, Staphylococcus* spp., *Proteus* spp., *Pseudomonas aeruginosa* and *Streptococcus* spp. (Helmy *et al.,* 2023). Catheter-associated urinary tract infections (CAUTIs) represent a significant portion of hospital-acquired illnesses, leading to increased patient morbidity, longer hospital stays, and heightened disease severity. Important to underline is the fact that the prolonged utilization of catheters not only raises healthcare expenses but also escalates the incidence of sickness and mortality. Approximately 70–80% of UTIs in hospitals are considered CAUTIs (Rubi *et al.,* 2022).

The two most crucial characteristics in developing novel biomaterials are antibacterial properties and biocompatibility. In the current study, a hydroxyapatite-gold-Cefuroxime nanocomposite was created by laser ablation that contains positively charged, hydrophilic Cefuroxime molecules that functionalize the surface of the Au, hydrophobic gold (Au) nanoparticles and hydroxyapatite (HAp). A composite material can be created using Hydroxyapatite biocompatibility and AuNPs' antibacterial ability to release NPs and Au ions. The main goal of this study is to create an affordable, efficient, and aqueous method for creating the Hydroxyapatite-Cefuroxime-Au composite and testing its efficacy against Gram-positive bacteria like *S. saprophyticus* that are linked to drug-resistant infections. Due to its ability to stop the growth of *S. saprophyticus* biofilms, it can be used as a preservative for Foley's catheter.

MATERIALS AND METHODS

Preparation and characterization of Hetero-structure nanoparticle: For the preparation of hetero nanostructure, we followed previous work (Yosif *et al.*, 2023).

***Staphylococcus saprophyticus* isolation:** A total of 25 *S. saprophyticus* isolates were obtained between December 2022 and February 2023 from 100 cases (urine and catheters) of UTIs at the Al-Kindi Hospital in Baghdad, Iraq. The Department of Applied Science at the University of Technology in Baghdad, Iraq, generously provided the VITEK system (Biomérieux, France), which was used to identify bacterial strains.

Antibacterial activity assay: The antibacterial efficacy of hydroxyapatite, Cefuroxime, AuNPs, hydroxyapatite-Cefuroxime, and hydroxyapatite-Cefuroxime-AuNPs was evaluated using the agar-well diffusion assay against *S. saprophyticus* strains (Khashan *et al.,* 2021). Sterile Petri dishes of 20 mL volume were aseptically filled with Muller-Hinton (MH) agar. By a sterile wire loop, the bacteria were removed from their stock cultures (Jihad *et al.,* 2021). After the organisms were cultured, the agar plates were drilled with a sterile point to create 6-mm-diameter wells. Hydroxyapatite, Cefuroxime, AuNPs, hydroxyapatite-Cefuroxime and hydroxyapatite-Cefuroxime-AuNPs were infused into the wells at varying concentrations. The samples were incubated at 37°C for 24 hr.

Fluorescence-activated cell sorting assay: LIVE/DEAD BacLight Bacterial Viability kit was used to color bacterial strains.

Biofilm test (Crystal violet assay): Grown bacterial strains in 96-well plates were administrated by the Hydroxyapatite NPs, cefuroxime, Au NPs, Hydroxyapatite-Cefuroxime, and Hydroxyapatite-Cefuroxime-AuNPs for 24 hours. The adhered bacteria were stained with 0.1% crystal violet (CV) before being twice rinsed with distilled water (DW). To quantify the growth of the biofilm, ethanol (0.2 ml, 95%) was supplemented to the CV-stained wells. Then, incubated for 2hr while being shaken. The optical density was measured at 595 nm (Jawad *et al.,* 2022).

Anti-Biofilm activity of Hertonanostructure: This is done to develop a biofilm on the Foley catheter, with a few changes from earlier studies (Hochbaum *et al.,* 2011). In brief, a catheter (1 cm x 1 cm) was placed in nutrient broth (9 ml) containing bacterial cell growth at a concentration of 1.5 $*10^5$ CFU/ml, which demonstrated the highest reduction in biofilm formation capacity after treatment with (Hydroxyapatite -Cefuroxime), (Au, Hydroxyapatite, Cefuroxime), and (AuNPs-Hydroxyapatite-Cefuroxime). Containers were aerobically incubated at 37°C for 24 hours. The adherent cells were given two washes by DW and were then given 30 minutes to dry. An atomic force microscope inspection of the catheter was prepared.

Cultivating the catheter in a nutrient broth without any attention or bacteria was used as the negative control. This was conducted alongside the cultivation of a catheter within a bacterial environment that was devoid of elements such as AuNPs, Hydroxyapatite, and Cefuroxime. Besides, it also included those free from Hydroxyapatite-Cefuroxime and AuNPs-Hydroxyapatite-Cefuroxime.

Statistical analysis: To statistically analyze the data, GraphPad Prism was used. The means and standard deviations from the three experiments are used to represent the data. Declare a statistically significant difference at $p \leq 0.05$ (Ali *et al.*, 2018; Al-Ziaydi *et al.*, 2020).

RESULTS

Characterization of Heterostructure of H.A-Anti-Au nanoparticles: The existence of nanoparticles was confirmed by the characteristics of (AuNPs-Hydroxyapatite-Cefuroxime) and (Au, Hydroxyapatite, and Cefuroxime) (Fig. 1). Hydroxyapatite-Cefuroxime, AuNPs, Hydroxyapatite, Cefuroxime, and AuNPs-Hydroxyapatite-Cefuroxime were put in a quartz cuvette, and distilled water served as the reference for measuring wavelength scanning (200-700 nm). Pure Cefuroxime, AuNPs, and HAP were discovered at 280, 525 and 200 nm, respectively. Hydroxyapatite-Cefuroxime-AuNPs and Hydroxyapatite-Cefuroxime revealed that the antibiotic exhibits the highest peak of absorption across all samples. This demonstrates that the antibiotic covered the substance's surface and consequently, the absorption intensity of the compound is higher than that of gold and hydroxyapatite. Optical energy bandgaps of the semiconductor were investigated by the given Tauc relationship (Gondal *et al.*, 2010):

$$(\alpha h\nu)1/n = K(h\nu - Eg)$$

Substances that possess an optical bandgap, Eg, denoted by n=1/2, permit direct transitions, whereas in materials with an optical bandgap, Eg and n signify 2, transitions are indirectly facilitated. The direct energy bandgap, Eg, can be discerned through the plotted graph of (αhν)2 against photon energy (hν), with the extrapolated line intersecting the axis representing photon energy at the position of the optical bandgap. The direct energy bandgaps of the Cefuroxime nanoparticles were 4.01 eV (Fig. 2-A), energy bandgaps of AuNPs in Fig. 2-B were 2.0 eV, while 5.01 eV for Hydroxyapatite in Fig. 2-C, Hydroxyapatite–Cefuroxime in Fig. 2-D were 4.04 eV, and eV of Hydroxyapatite-Cefuroxime-AuNPs were 4.03 in Fig. 2-E. The surface morphology and particle size of the heterostructure composite synthesized using laser ablation were determined by FESEM analysis. Fig. 3(A) explains the FESEM images of Hydroxyapatite-cefuroxime, AuNPs, Hydroxyapatite NPs, and Hydroxyapatite-cefuroxime-Au. The histogram size distribution of Au NPs was 30nm, Hydroxyapatite NPs was 36nm, Hydroxyapatite-Cefuroxime was 53nm and for Hydroxyapatite–Cefuroxime - Au was 66nm (Fig. 3B).

From these results, we can explain the method of attachment or packaging of this compound through the size of the particles, where the gold is coated with hydroxyapatite and the antibiotic encapsulates them from the outside and this is consistent with the results of the UV.

Isolates of *S. saprophyticus*: There was a total of 25 isolates of *S. saprophyticus*, which were obtained from urine and catheters of UTIs cases (60% (n=15) and 40% (n=10), respectively).

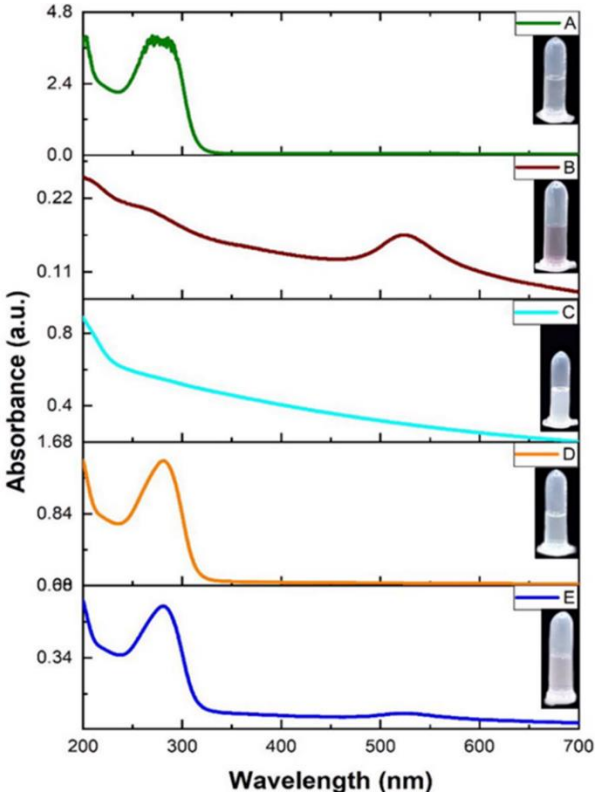

Fig. 1: UV of A, (Cefuroxime). B, (Au NPs). C, (Hydroxyapatite NPs). D, (Hydroxyapatite-Cefuroxime). E, (Hydroxyapatite-Cefuroxime-AuNPs).

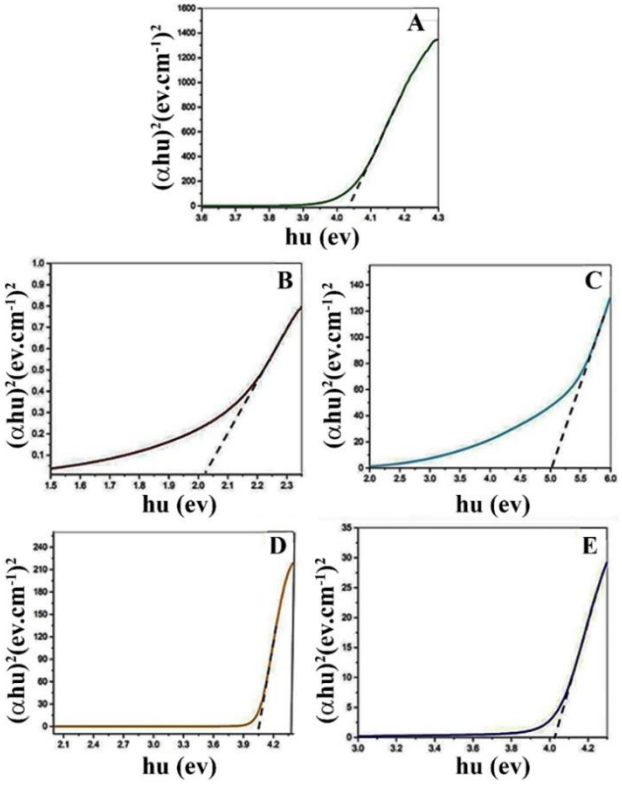

Fig. 2: The energy gap of A, (Cefuroxime). B, (Au NPs). C, (Hydroxyap atite). D, (Hydroxyapatite-Cefuroxime). E, ((Hydroxyapatite-Cefuroxime-AuNPs).

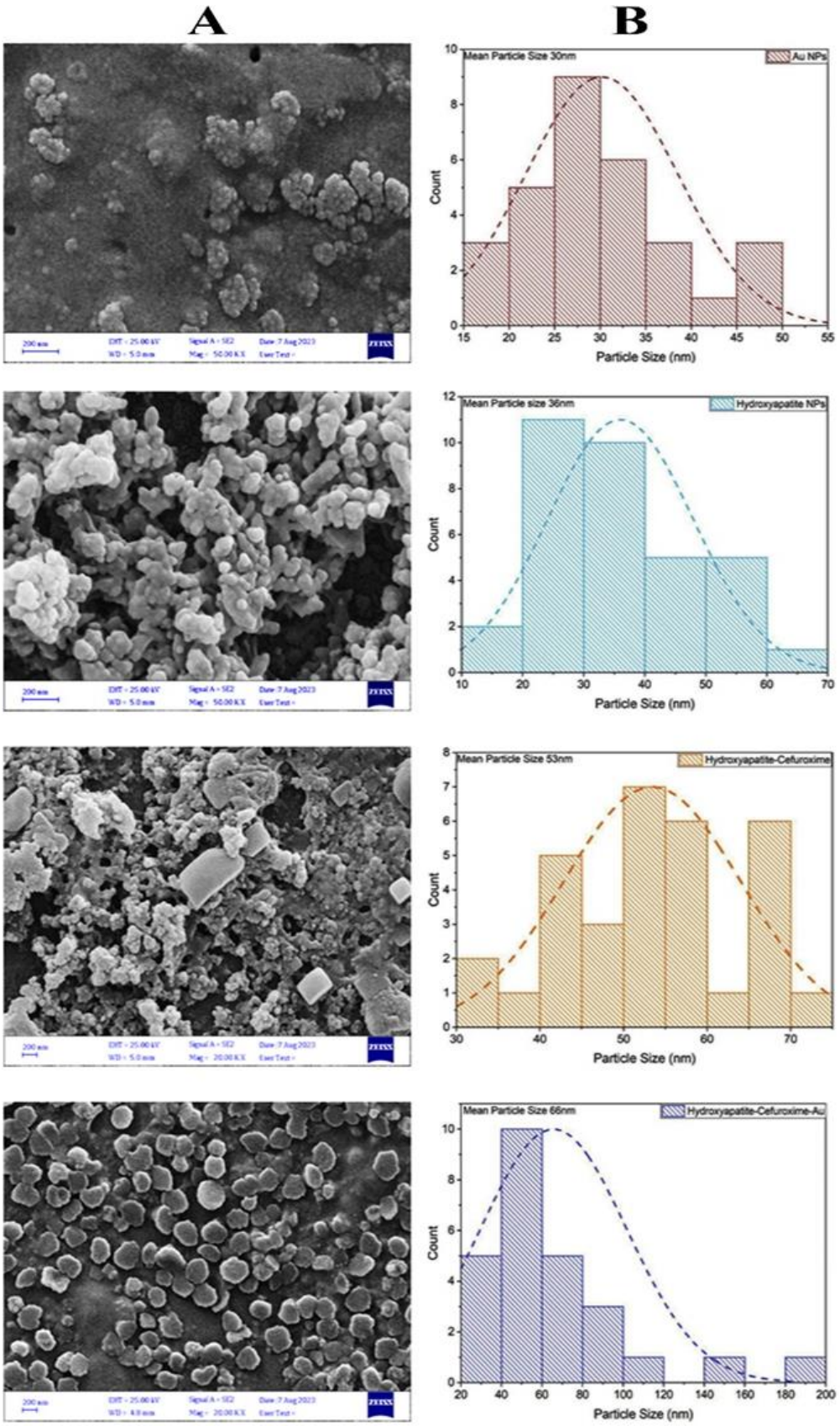

Fig. 3: FESEM of (A) Au NPs, Hydroxyapatite NPs, Hydroxyapatite NPs-Cefuroxime, Hydroxyapatite-Cefuroxime-Au prepared by laser ablation 1064 nm. (B) Histogram of Particle Size.

Antibiotics susceptibility test: According to the results of the present study, *S. saprophyticus* isolates were highly resistant to Amoxillin (75%), Ceftazidem (66%), cefuroxime (67%), and Narfloaxcin (65%), as well as low levels of resistance to Impenem (0%) and Amikacin (25%), Cefotaxime (26%), Ceflxime (27%), Ciprofloxacin (35%), Carbenicllin (50%) as indicated in Fig. 4.

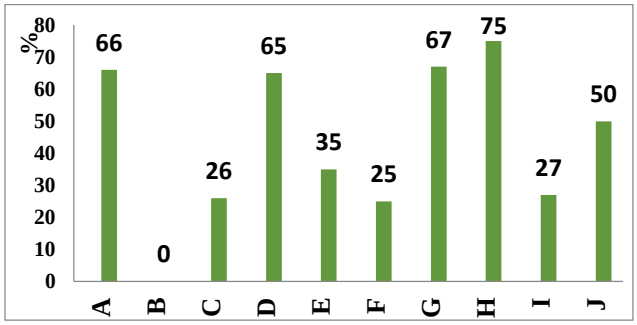

Fig. 4: Antibiotic susceptibility of *Staphylococcus saprophyticus* isolates. (A, Ceftazidem), (B, Imipenem), (C, Cefotaxime), (D, Narfloaxcin), (E, Ciprofloxacine), (F, Amikacin), (G, Cefuroxime), (H, Amoxillin Clavul), (I, Ceflxime), (J, Carbenicllin).

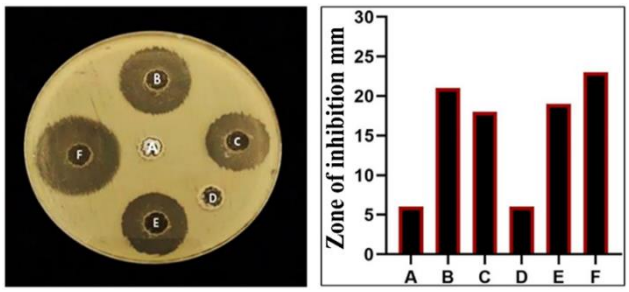

Fig. 5: Antibacterial activity against *Staphylococcus saprophyticus.* A, (control). B, (Cefuroxime). C, (Au NPs). D, (HAP NPs). E, (HAP NPs-Cefuroxime). F, (HAP NPs- Cefuroxime -AuNPs).

Synergistic effect of tested materials against *S. saprophyticus:* The synergistic antimicrobial effects of the HydroxyapatiteNPs, Cefuroxime antibiotic, AuNPs, HydroxyapatiteNPs-Cefuroxime, and HydroxyapatiteNPs-Cefuroxime-AuNPs on the *S. saprophyticus* isolates growth were compared to that of the HydroxyapatiteNPs, Cefuroxime antibiotic and AuNPs alone. The results showed an increase of Cefuroxime antibiotic effects on all evaluated bacteria when conjugated with AuNPs and HydroxyapatiteNPs. The greatest synergistic effect was detected for the HydroxyapatiteNPs-Cefuroxime-AuNPs (Fig. 5). There was an increase in the diameter of the inhibition zones of the bacterial strains that demonstrated the synergistic effects of the tested materials. The inhibition zone of HydroxyapatiteNPs alone was 6nm, AuNPs was 16 mm, while that of Cefuroxime alone was 19 mm, respectively. The inhibition zone of HydroxyapatiteNPs-Cefuroxime antibiotic was 17 mm, while in HydroxyapatiteNPs-Cefuroxime antibiotic-AuNPs, the largest inhibition area 22 mm was obtained for *S. saprophyticus*. There was an increase in the sensitivity of *S. saprophyticus* to Cefuroxime after its loading onto the AuNPs and HydroxyapatiteNPs. The inhibition zone increased to ~27 mm for the HydroxyapatiteNPs-Cefuroxime antibiotic-AuNPs from 19 mm with Cefuroxime alone, which caused the cell lysis via interfering with the bacterial cell wall.

Viability assay: The bactericidal activity of the hetero-nano composite was further validated by conducting viability tests on bacteria using flow cytometry. Two types of DNA-binding pigments, SYTO9 and Propidium Iodide (PI), were utilized in this analysis due to their distinct cell penetration capabilities. It's important to note that SYTO9 can penetrate both living and deceased cells, presenting a contrast to PI. The latter is only capable of infiltrating cells once the integrity of their membrane is compromised, namely when the cells are in a state of death or being killed. Compared to traditional plate analysis, the use of flow cytometry proves more effective in identifying dead or dying bacterial cells. This is largely due to its rapid detection of a loss in bacterial cell permeability through the use of Propidium Iodide (PI) incorporation. At the start of the experiment, tests were conducted to measure the initial percentage of PI-positive cells. Following treatment with the materials under investigation for six hours, the viability of the bacterial types was then determined. These materials were found to cause the most cell death, as evidenced by the rate of PI-positive bacterial cells (Fig. 6).

Anti-biofilm activity of hetero nanostructure: HydroxyapatiteNPs, Cefuroxime antibiotic, AuNPs and their combinations were tested to analyze their impacts on biofilm formation in the lab. The study involved assessing how the crystal violet (CV) formula binds to cells that adhere, directly demonstrating the efficiency of these mixtures in inhibiting biofilms. The assessment using 0.1% CV staining indicated the tested bacteria's biofilm production potential, suggesting the high resistance to most formulations such as HydroxyapatiteNPs, Cefuroxime antibiotic, AuNPs, and their nanocomposite. Yet, it was apparent that nanoconjugates effectively eradicated the biofilm when used for treatment. The results showed that HydroxyapatiteNPs-Cefuroxime-AuNPs nanoconjugate had the most potent inhibitory effect (Fig. 7).

AFM at the Foley catheter was utilized to assess the potency of various solutions including the cefuroxime antibiotic, Au NPS, hydroxyapatite NPs, Hydroxyapatite-Cefuroxime, and Hydroxyapatite-Cefuroxime-Au at inhibiting biofilm production. However, the efficacy of Hydroxyapatite-Cefuroxime-Au at halting the growth of biofilm on the Foley catheter was found to be comparatively less. The biofilm growth results from an AFM test on a catheter in Figure 8A depict the absence of microorganisms and the presence of a biofilm with a diameter of 600 nm. While the catheter containing *S. saprophyticus* bacteria was 1200 nm Fig. 8B and 8C show the surface after treatment of *S. saprophyticus* with Cefuroxime almost 830 nm., Fig. 8D shows the surface after treatment of *S. saprophyticus* by Au NPS it was 819 nm. *S. saprophyticus* was present on the lower surface, and it was treated with Hydroxyapatite NPs at an 1148 nm wavelength Fig. 8E, whereas *S. saprophyticus* was present on the upper surface and it was treated with Hydroxyapatite –Cefuroxime at an 822 nm wavelength Fig. 8F. The largest surface measurement was 677 nm Fig. 8G when *S. saprophyticus* and Hydroxyapatite –Cefuroxime-Au were combined. According to these results, cefuroxime antibiotics alone were not as effective at preventing biofilm as Hydroxyapatite–Cefuroxime-AuNPs composites.

DISCUSSION

S. saprophyticus was one of the most commonly non-aureus *Staphylococcus* species isolated from dairy cows that suffered from mastitis in many countries (Vanderhaeghen *et al.*, 2014; Goetz *et al.*, 2017; Jenkins *et al.*, 2019; Qu *et al.*, 2019; Shoaib *et al.*, 2023).

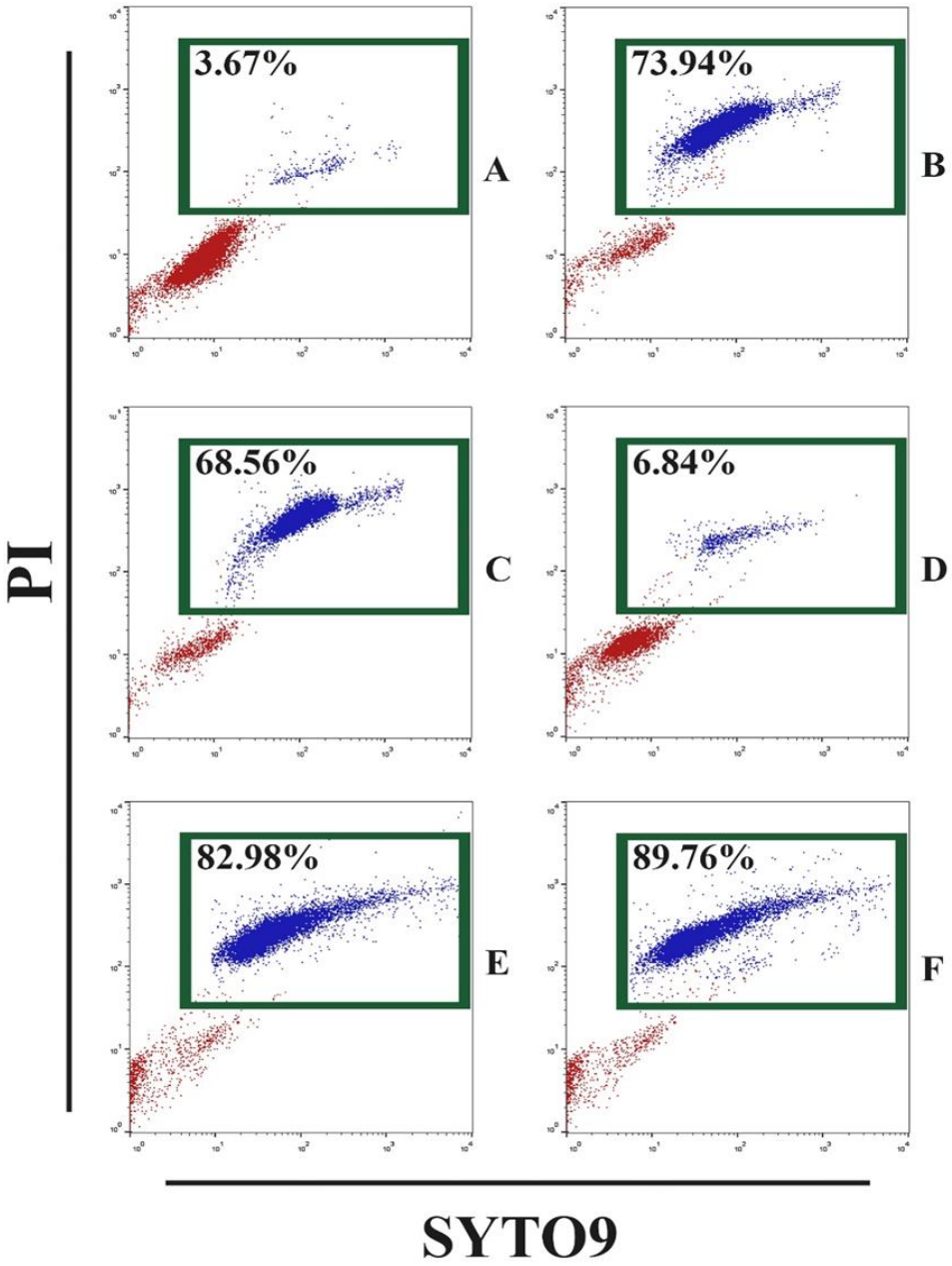

Fig. 6: Effect of tested materials on viability of *S. saprophyticus*. Microbial strains were treated with tested materials for 24 hours and stained with PI and SYTO9. A, (control). B, (Cefuroxime). C, (Au NPs). D, (H.A NPs). E, (H.A NPs- Cefuroxime). F, (H.A NPs- Cefuroxime -AuNPs).

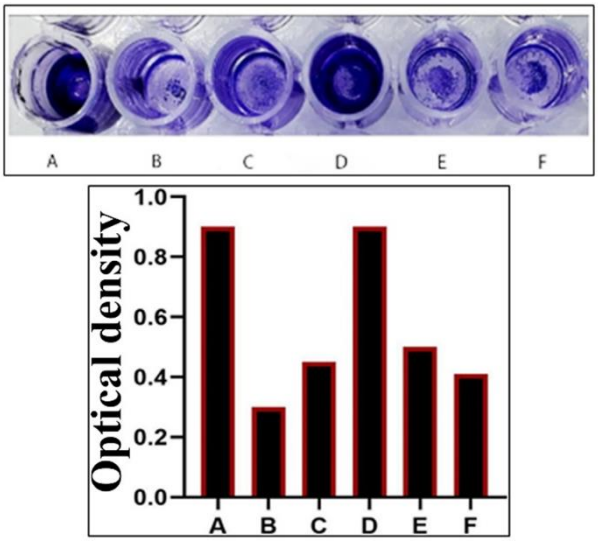

Fig. 7: Reduction of biofilm formation of *Staphylococcus saprophyticus*. A, (control). B, (Cefuroxime). C, (Au NPs). D, (H.A NPs). E, (H.A NPs- Cefuroxime). F, (H.A NPs- Cefuroxime -AuNPs).

This research affirmed that the heterogeneous nanocomposite displayed superior antimicrobial activity against *S. saprophyticus* than Cefuroxime alone. The advanced hybrid nanomaterials have showcased promising results, suggesting their potential efficacy in combating *S. saprophyticus* and offering a sound tactic for preventing bacterial biofilm formation in future instances of urinary tract infections. Various microorganisms such as *Proteus mirabilis, Escherichia coli, S. saprophyticus, Klebsiella pneumoniae* and *Enterococcus faecalis* are recognized causes of UTIs. The present study reveals that *S. saprophyticus* is evolving resistance to commonly used antibiotics, a response likely driven by the pressure antibiotic overuse places on particular microorganisms already in existence. The extent of the detected resistance was quite surprising. Fluoroquinolones are a category of antibiotics encompassing drugs like ciprofloxacin and norfloxacin. They are multipurpose synthetic antibiotics. The primary purpose of gram-positive bacteria is to restrict the activity of topoisomerase II (DNAase), which

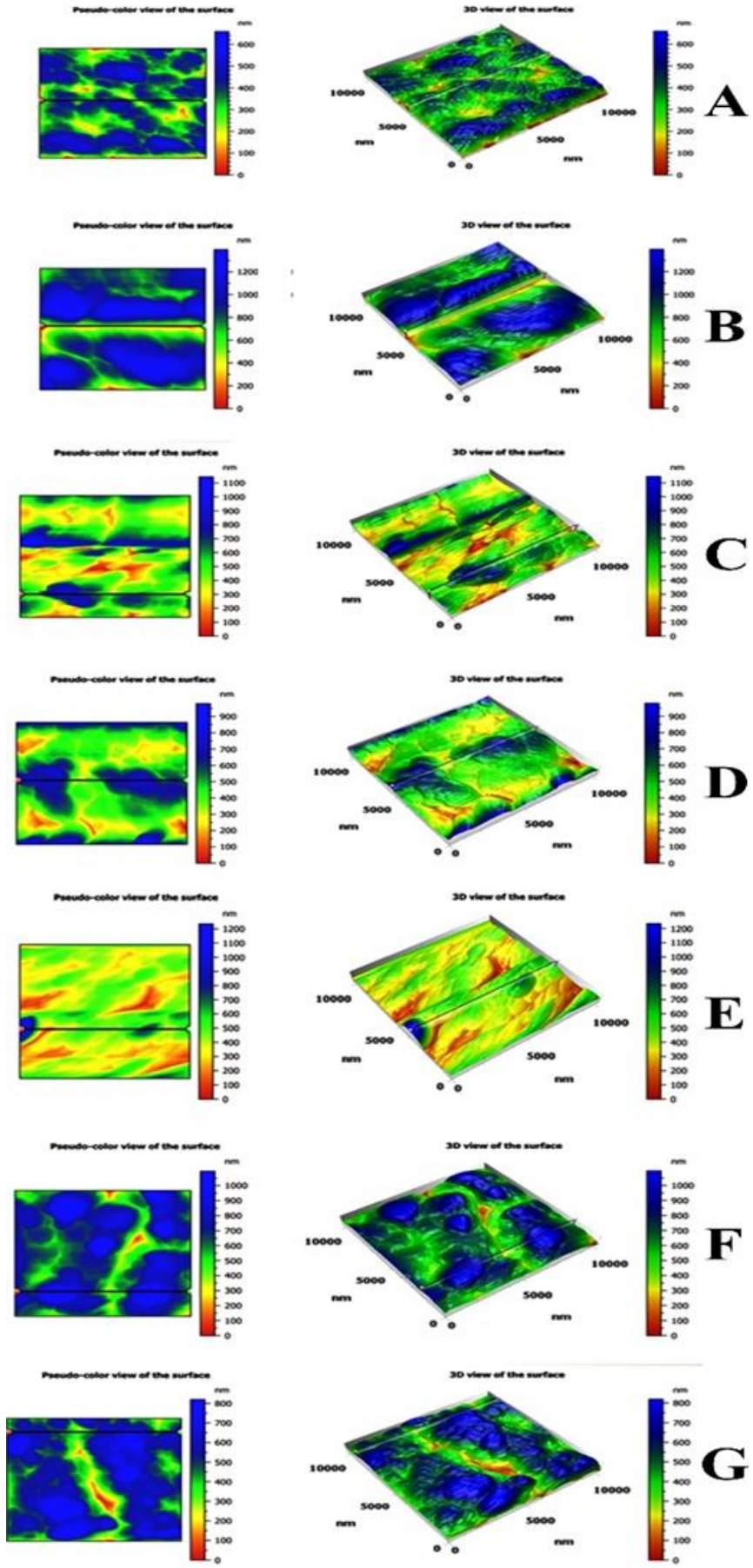

Fig. 8: Anti-biofilm activity of hetero nanostructure conjugated Cefuroxime in Foley's catheter (A) Foley's catheter only, (B) *Staphylococcus saprophyticus* only, *(C)* Cefuroxime treated bacterial strains, (D) Au NPS treated bacterial strains, (E) Hydroxyapatite NPs treated bacterial strains, (F) Hydroxyapatite–Cefuroxime treated bacterial strains, (G) Hydroxyapatite-Cefuroxime-AuNPs treated bacterial strains.

fluoroquinolones accomplish by inhibiting DNA replication. The emergence of resistance to different classes of antibiotics can usually be attributed to various factors. These include changes in the structure of the target site, modifications in the permeability of the cell membrane and the functioning of efflux pump mechanisms that reduce antibiotic concentrations (Jabir *et al.*, 2022). Because there are so few new antimicrobial drugs being developed, the issue of rising antibiotic resistance is very concerning (Prestinaci *et al.*, 2015). By conjugating gold nanoparticles (AuNPs) and Hydroxyapatite nanoparticles (NPs) with Cefuroxime, the entry of antibiotics into bacterial cells is enhanced. As reported, these combinations block the activities of DNA gyrase enzyme and topoisomerase IV, thus obstructing cell division and eventually causing bacterial cell death (Mala *et al*., 2012; Nikparast and Saliani, 2018). When these nanoparticles are combined with antibiotics, less amount of the drug is needed, consequently reducing its toxicity and the possibility of bacterial resistance development (Zhou *et al*., 2016). Moreover, evidence from the 0.1% CV staining assay indicates the ability of the tested bacteria to generate a biofilm, explaining the high resistance rate found in a majority of the formulations, i.e., HydroxyapatiteNPs, Cefuroxime antibiotic, AuNPs, HydroxyapatiteNPs-Cefuroxime, and HydroxyapatiteNPs-Cefuroxime-AuNPs. However, when treated with HydroxyapatiteNPs, Cefuroxime antibiotic, AuNPs, and their conjugates, the results highlighted the effective removal of the biofilm by nanoconjugates. In terms of the most potent inhibition effect, the HydroxyapatiteNPs-Cefuroxime-AuNPs nanoconjugate emerged as the standout. A summary of all results regarding *S. saprophyticus* treated with the materials tested is outlined in Figure 8. The nanoparticles (NPs) seem to affect the biofilm formation in the bacteria by infiltrating the bacterial cell and disrupting the essential proteins and enzymes needed for microbial adhesion. This action leads to a reduction in biofilm formation as the NPs work to hinder the development of external polysaccharides, commonly referred to as exopolysaccharides. Additionally, the biofilm formation process is further inhibited by NPs when they penetrate the water channels, or Aqua pores, responsible for carrying water and nutrients through the layers of polysaccharides on the bacterial cell wall (Ahire *et al*., 2015). A previous study by (Silva-Holguín and Reyes-López, 2020), demonstrated that the HAp-AgNPs composites which are prepared by the sol-gel method have excellent antibacterial activity against variety of bacterial strains at different concentrations.

Conclusions: In this study, the laser ablation technique is successfully used to create heterostructure nanoparticles of the Hydroxyapatite-Cefuroxime-AuNPs. The FESEM image demonstrates the spherical structure of Au, and Hydroxyapatite nanoparticles alone with mean sizes of 30 nm. However, the heterostructure composite demonstrates an increase in size for Hydroxyapatite-Cefuroxime-Au to 66 nm. The Hydroxyapatite nanoparticles (NPs)-Cefuroxime-Gold nanoparticles (AuNPs) hybrid was developed as an intelligent drug delivery mechanism to prevent the proliferation of *S. saprophyticus* and to hinder the formation of bacterial biofilm on Foley catheters. The overarching outcomes of the study highlighted that the AuNPs, when covered with Hydroxyapatite NPs, functioned adequately as a vehicle for Cefuroxime delivery. The current study's findings underlined that the antimicrobial properties of these heterostructure nanocomposites provide a multitude of opportunities for their use as potent and effective antibiotics in clinical treatments. This marks them as a promising part of cutting-edge Nanomedicine for future applications.

Acknowledgments: The authors extend their appreciation to the Researchers Supporting Project number (RSPD2024R971), King Saud University, Riyadh, Saudi Arabia for funding this research. The authors appreciated the University of Technology, Iraq, for the logistic support of this work.

Authors contribution: Hadeel M. Yosif and Majid S. Jabir were responsible for developing the initial draft, driving the methodology, undertaking the investigation, and performing formal analyses. Buthenia A. Hasoon and Majid S. Jabir oversaw the main conceptual work, data interpretation, and supervision. Syed Hilal Yaqoob, Hani Samir, and Ayman A. Swelum contributed to the writing review, editing processes, visualization, and data organization. The manuscript was reviewed by every author.

Data availability: Not applicable.

Declarations

Funding: The Researchers Supporting Project number (RSPD2024R971), King Saud University, Riyadh, Saudi Arabia funded this research.

Conflict of interest: The authors declare no competing interests.

REFERENCES

Abbas R, Nawaz Z, Siddique AB, *et al*., 2022. Molecular detection of biofilm production among multidrug resistant isolates of *Pseudomonas aeruginosa* from meat samples. Pak Vet J 42:505-510.

Ahire JJ, Neveling DP, Hattingh M, *et al.,* 2015. Ciprofloxacin-eluting nanofibers inhibit biofilm formation by *Pseudomonas aeruginosa* and a methicillin-resistant *Staphylococcus aureus*. PLoS One 10:e0123648.

Ahmed A, Ijaz M, Khan JA, *et al*., 2022. Molecular characterization and therapeutic insights into biofilm positive *Staphylococcus aureus* isolated from bovine subclinical mastitis. Pak Vet J 42(4):584-590.

Ali IH, Jabir MS, Al-Shmgani HS, *et al.,* 2018. May. Pathological and immunological study on infection with *Escherichia coli* in ale balb/c mice. | Physics:Conference Series 1003:012009.

Al-Ziaydi AG, Al-Shammari AM, Hamzah MI, *et al*., 2020. Hexokinase inhibition using D-Mannoheptulose enhances oncolytic Newcastle disease virus-mediated killing of breast cancer cells. Cancer Cell Int 20:1-10.

Cassandra W, 2017. The drug-resistant bacteria that pose the greatest health threats. Nature 543:15.

De Buck J, Ha V, Naushad S, *et al*., 2021. Non-aureus staphylococci and bovine udder health:current understanding and knowledge gaps. Front Vet Sci 8:658031. doi:10.3389/fvets.2021.658031

Flores-Mireles AL, Walker JN, Caparon M, *et al*., 2015. Urinary tract infections:epidemiology, mechanisms of infection and treatment options. Nat Rev Microbiol 13(5):269-284.

Goetz C, Tremblay YD, Lamarche D, *et al.,* 2017. Coagulase-negative staphylococci species affect biofilm formation of other coagulase-negative and coagulase-positive staphylococci. J Dairy Sci 100(8):6454–6464. doi:10.3168/jds.2017-12629

Gondal MA, Drmosh QA and Saleh TA, 2010. Preparation and characterization of SnO_2 nanoparticles using high power pulsed laser. Applied Surface Sci 256:7067-7070.

Rubi H, Mudey G and Kunjalwar R, 2022. Catheter-Associated Urinary Tract Infection (CAUTI). Cureus 14(10):e30385. doi:10.7759/cureus.30385

Hassan H, Sharma P, Hasan MR, *et al*., 2022. Gold nanomaterials–The golden approach from synthesis to applications. Mater Sci Energy Technol 5:375-390. doi:10.1016/j.mset.2022.09.004

Helmy AK, Sidkey NM, El-Badawy RE, *et al*., 2023. Emergence of microbial infections in some hospitals of Cairo, Egypt: studying their corresponding antimicrobial resistance profiles. BMC Infect Dis 23(1):1-13.9

Hochbaum AI, Kolodkin-Gal I, Foulston L, *et al.,* 2011. Inhibitory effects of D-amino acids on *Staphylococcus aureus* biofilm development. J Bacteriol, 193(20) 5616-5622.

Jabir MS, Rashid TM, Nayef UM, *et al.,* 2022. Inhibition of Staphylococcus aureus α-hemolysin production using nanocurcumin capped Au@ ZnO nanocomposite. Bioinorganic Chem Appl 2022:2663812. doi:10.1155/2022/2663812

Jawad KH, Marzoog TR, Hasoon BA, *et al.,* 2022. Antibacterial activity of bismuth oxide nanoparticles compared to amikacin against *Acinetobacter baumannii* and *Staphylococcus aureus*. J Nanomaterials 2022:8511601. doi:10.1155/2022/8511601

Jenkins SN, Okello E, Rossitto PV, *et al.,* 2019. Molecular epidemiology of coagulase-negative *Staphylococcus* species isolated at different lactation stages from dairy cattle in the United States. PeerJ 7:e6749. doi:10.7717/peerj.6749

Jihad MA, Noori FT, Jabir MS, *et al.,* 2021. Polyethylene glycol functionalized graphene oxide nanoparticles loaded with nigella sativa extract: a smart antibacterial therapeutic drug delivery system. Molecules 26:3067.

Kaul S, Gulati N, Verma D, *et al.,* 2018. Role of nanotechnology in cosmeceuticals: a review of recent advances. J Pharm 2018:3420204.

Khashan KS, Abdulameer FA, Jabir MS, *et al.,* 2020. Anticancer activity and toxicity of carbon nanoparticles produced by pulsed laser ablation of graphite in water. Adv in Nat Sci: Nanosci Nanotech 11:035010.

Khashan KS, Badr BA, Sulaiman GM, *et al.,* 2021. Antibacterial activity of Zinc Oxide nanostructured materials synthesis by laser ablation method. In J Phys: Conference Series 1795:012040.

Koch G, Yepes A, Förstner KU, *et al.,* 2014. Evolution of resistance to a last-resort antibiotic in Staphylococcus aureus via bacterial competition. Cell 158:1060-1071.

Liu J, Zhang X, Niu J, *et al*., 2023. Complete Genome of Multi-Drug Resistant *Staphylococcus aureus* in Bovine Mastitic Milk in Anhui, China. Pak Vet J 43(3):456-462.

Makabenta JMV, Nabawy A, Li CH, *et al.,* 2021. Nanomaterial-based therapeutics for antibiotic-resistant bacterial infections. Nat Rev Microbiol 19:23-36.

Mala R, Arunachalam P and Sivasankari M, 2012. Synergistic bactericidal activity of silver nanoparticles and ciprofloxacin against phytopathogens. I Cell Tissue Res 12:3249.

Mancuso G, Midiri A, Gerace E, *et al*., 2023. Urinary tract infections: The current scenario and future prospects. Pathogens 12(4):623.

Naima A, Aqib AI, Akram K, *et al*., 2022. Resistance modulation of dairy milk borne *Streptococcus agalactiae* and *Klebsiella pneumoniae* through metallic oxide nanoparticles. Pak Vet J 42(3):424-428.

Naylor NR, Atun R, Zhu N, *et al.,* 2018. Estimating the burden of antimicrobial resistance: a systematic literature review. Antimicrob Resist Infect Control 7:1-17.

Nicolle LE, 2005. Catheter-related urinary tract infection. Drugs Aging 22:627-639.

Nikparast Y and Saliani M, 2018. Synergistic effect between phyto-syntesized silver nanoparticles and ciprofloxacin antibiotic on some pathogenic bacterial strains. J Med Bacteriol 7:36-43.

Patel H, Wu ZX, Chen Y, *et al.,* 2021. Drug resistance: From bacteria to cancer. Mol Biomed 2:1-19.

Prestinaci F, Pezzotti P and Pantosti A, 2015. Antimicrobial resistance:a global multifaceted phenomenon. Pathog Glob Health 109:309-318.

Qu Y, Zhao H, Nobrega DB, *et al.,* 2019. Molecular epidemiology and distribution of antimicrobial resistance genes of *staphylococcus* species isolated from Chinese dairy cows with clinical mastitis. J Dairy Sci 102 (2):1571–1583. doi:10.3168/jds.2018-15136

Raj S, Jose S, Sumod US, *et al.,* 2012. Nanotechnology in cosmetics: Opportunities and challenges. J Pharmacy & Bioallied Sci 4(3):186.

Shoaib M, Xu J, Meng X, *et al.,* 2023. Molecular epidemiology and characterization of antimicrobial-resistant *Staphylococcus haemolyticus* strains isolated from dairy cattle milk in Northwest, China. Front Cell Infect Microbiol 13:1183390. doi:10.3389/fcimb.2023.1183390

Silva-Holguín PN and Reyes-López SY, 2020. Synthesis of Hydroxyapatite-Ag composite as antimicrobial agent. Dose Response. 4:18(3):1559325820951342.

Stamm WE and Norrby SR, 2001. Urinary tract infections: disease panorama and challenges. J Infectious Dis 183(Supplement_1):S1-4.

Tian B, Chen, W, Dong Y, *et al.,* 2016. Silver nanoparticle-loaded hydroxyapatite coating: structure, antibacterial properties, and capacity for osteogenic induction in vitro. RSC Adv 6:8549-8562.

Vanderhaeghen W, Piepers S, Leroy F, *et al.,* 2014. Invited review: effect, persistence, and virulence of coagulase-negative *staphylococcus* species associated with ruminant udder health. J Dairy Sci 97 (9):5275–5293. doi:10.3168/jds.2013-7775

Vila JORDI, Moreno-Morales J and Ballesté-Delpierre C, 2020. Current landscape in the discovery of novel antibacterial agents. Clin Microbiol Infect 26:596-603.

Wald R, Hess C, Urbantke V, *et al.*, 2019. Characterization of *Staphylococcus* species isolated from bovine quarter milk samples. Animals 9 (5):200. doi:10.3390/ani9050200

Willyard C, 2017. Drug-resistant bacteria ranked. Nature, 543:15.

Yosif HM, Hasoon BA and Jabir MS, 2023. Laser Ablation for Synthesis of Hydroxyapatite and Au NP Conjugated Cefuroxime:Evaluation of Their Effects on the Biofilm Formation of Multidrug Resistance *Klebsiella pneumoniae*. Plasmonics 2023. doi:10.1007/s11468-023-02053-y

Yuan Q, Xu A, Zhang Z, *et al.,* 2018. Bioactive silver doped hydroxyapatite composite coatings on metal substrates: synthesis and characterization. Materials Chem Phys 218:130-139.

Zhang WH, Shi JL, Wang LZ, *et al.,* 2000. Preparation and characterization of ZnO clusters inside mesoporous silica. Chem of Mat 12:1408-1413.

Zhang XF, Liu ZG, Shen W, *et al*., 2016. Silver nanoparticles: synthesis, characterization, properties, applications, and therapeutic approaches. Int J Mol Sci 17:1534.

Zhou XH, Wei DX, Ye HM, *et al.,* 2016. Development of poly (vinyl alcohol) porous scaffold with high strength and well ciprofloxacin release efficiency. Mater Sci Eng C 67:326-335.